RRB-88-25

DETERMINATION OF IRRADIATION AND PRIMARY PRODUCTION USING A TIME-DEPENDENT ATTENTUATION COEFFICIENT

by
R.P. Bukata, J.H. Jerome
and J.E. Bruton

Rivers Research Branch
National Water Research Institute
Canada Centre for Inland Waters
Burlington, Ontario, Canada L7R 4A6

May 1988
NWRI Contribution #88-85

MANAGEMENT PERSPECTIVE

It is evident that an institute such as NWRI/CCIW dedicated to the protection and conservation of natural waters is concerned with the photosynthetic processes occurring within the water column. As such, both in situ measurements and mathematical modelling estimates of primary production and subsurface irradiation comprise vital and continual activities. This work utilizes Monte Carlo computer simulations of photon propagation through a variety of water types in conjunction with the Vollenweider-Fee primary production model to evaluate the impact of the diurnal variation of solar zenith angle on estimates of both primary production and irradiation for several different geographic locations and times of year.

It is shown that the impact of ignoring the diurnal solar zenith angle variation is not substantial (<±15%) on primary production estimates, but can be quite substantial (as high as ±80% under certain conditions of latitude and season) on in situ determinations of subsurface irradiation.

SOMMARE POUR LA GESTION

Il va de soi qu'un établissement comme le INRE/CCEI voué à la protection et à la conservation des eaux naturelles s'intéresse aux processus de photosynthèse survenant dans la colonne d'eau. A cet égard, le mesurage in situ et l'estimation par modélisation mathématique de la production primaire et de l'irradiation subsurfacique constituent des tâches vitales et continues. Dans le présent travail, on se sert de simulations informatiques de Monte Carlo de la propagation des photons dans diverses eaux ainsi que du modèle de production primaire Vollenweider-Fee pour évaluer les effets de la variation diurne de l'angle zénithal solaire sur les estimations de la production primaire et de l'irradiation, à plusieurs endroits et moments de l'année.

On montre que négliger cette variation diurne n'a pas un grand effet (±15 %) sur l'estimation de la production primaire, mais que selon la latitude et la saison, les écarts peuvent atteindre 80 % dans le cas de la détermination in situ de l'irradiation subsurfacique.

ABSTRACT

A time-dependent vertical irradiance attenuation coefficient $k_v(\theta_r)$ is utilized in conjunction with the Vollenweider-Fee primary production model to determine the effect of the diurnal variation of solar zenith angle on estimations of primary production and irradiation. Such effects are considered as a function of both geographic latitude (northern hemisphere) and time of year. It is shown that the effect of solar zenith angle dependence of the vertical irradiance attenuation coefficient on the determination of daily primary production is small (<±15%) for any latitude or time of year. The effect of solar zenith angle dependence of the vertical irradiance attenuation coefficient on the determination of irradiation at a given depth, however, can be quite significant. Under certain conditions of latitude and time, this effect can be as large as ±80%.

RÉSUMÉ

On utilise un coefficient d'atténuation de l'irradiance verticale à dépendance temporelle, $k_v(\theta_r)$, avec le modèle de production primaire Vollenweider-Fee afin de déterminer les effets de la variation diurne de l'angle zénithal solaire sur les estimations de la production primaire et de l'irradiation. On pense généralement que ces effets sont fonction à la fois de la latitude géographique (hémisphère nord) et de la période de l'année. Il est montré que l'effet de dépendance envers l'angle zénithal solaire du coefficient d'atténuation de l'irradiance verticale sur la détermination de la production primaire quotidienne est petit (<15 %), pour toute latitude et pour toute période de l'année. Mais il peut être assez important pour ce qui est de la détermination de l'irradiation à une profondeur donnée : il peut atteindre 80 % sous certaines latitudes et à certaines périodes.

INTRODUCTION

One of the most significant parameters governing the photosynthetic processes in natural water bodies is the daily integrated value of subsurface irradiance within the water column. Various models have been proposed for mathematically estimating primary production, among the most notable being those of Smith (1936), Talling (1957), Vollenweider (1965), and others reviewed in Vollenweider (1965) and Patten (1968). Fee (1969) has presented a numerical solution of the Vollenweider photosynthesis model which enables an exploitation of its full generality. In this paper we utilize the Fee numerical solution in conjunction with the realistic diurnal variation of the vertical irradiance attenuation coefficient to determine the accuracy to which daily integrated values of primary production are presently estimated. The diurnal variation of the vertical irradiance attenuation coefficient is also used to determine the accuracy to which daily integrated values of subsurface irradiance (i.e., irradiation) are presently estimated.

The value of the vertical irradiance attenuation coefficient is dependent upon not only the inherent optical properties (absorption and scattering) of the various components of natural waters and the nature of the incident radiation distributions, but also the solar zenith angle at the time subsurface irradiance profiling is performed to determine the attenuation coefficient.

Figure 1 schematically illustrates in ray form the path of an incident beam (solar zenith angle θ_i, refracted angle θ_r) entering the water. Z_L (θ_r) is the path length along the principal direction of subsurface propagation to a particular irradiance level. Z is the vertical distance to that level.

The general expression for the attenuation of subsurface irradiance is Beer's Law, which may be expressed as

$$E(Z,\theta_r) = E(0,\theta_r)\exp(-kZ_L(\theta_r)) \qquad (1)$$

where $E(Z,\theta_r)$ = irradiance at depth Z

$E(0,\theta_r)$ = irradiance just beneath the surface

k = irradiance attenuation coefficient

θ_r = in-water refracted angle

= arcsine $(0.75 \sin(\theta_i))$

Replacing Z_L by the vertical depth Z in equation (1) yields

$$E(Z,\theta_r) = E(0,\theta_r)\exp(-k_v(\theta_r)Z) \qquad (2)$$

where $k_v(\theta_r)$ = vertical irradiance attenuation coefficient.

Since $Z = Z_L$ only for the condition of the sun directly overhead (i.e., $\theta_i = \theta_r = 0$), the experimentally-determined value of the vertical irradiance attenuation coefficient varies with the time at which the subsurface irradiance profile is performed. Extending the use of an invariant $k_v(\theta_r)$ throughout the daylight hours, therefore, defines an inappropriate diurnal variation for the subsurface irradiance levels $E(Z,\theta_r)$.

METHODOLOGY

Figure 2 illustrates a flow diagram of the mathematical methodologies utilized in this work. Various incident radiation fields, water types, and temporal and spatial parameters are used to determine $k_v(\theta_r)$, the vertical irradiance attenuation coefficient, as a function of solar zenith angle. These $k_v(\theta_r)$ values are then utilized in a two-fold manner. They are used, in conjunction with the Vollenweider primary production model parameters and the Fee integration technique to evaluate the relative over/under estimation of primary production introduced by neglecting the diurnal variation of $k_v(\theta_r)$. The $k_v(\theta_r)$ values are then used to determine subsurface irradiance levels as a function of depth. Following integration of these irradiance levels over the daylight period, the relative over/under estimation of subsurface irradiation introduced by neglecting the diurnal variation of $k_v(\theta_r)$ is calculated.

a) Determination of Primary Production

The incident radiation field (atmospheric model described in Appendix A), the natural water type (defined in terms of its scattering albedo ω and its absorption coefficient a), and the time and geographic space parameters (solar zenith angle θ_i and latitude °N, for a variety of Julian days) are used as inputs to the empirical

equations given in Kirk (1984) to determine the diurnal variation of $k_v(\theta_r)$. The details of these determinations are given in Appendix B. These values of $k_v(\theta_r)$ along with suitable values of the parameters from the Vollenweider (1965) model serve as inputs to the Vollenweider-Fee (Vollenweider, 1965; Fee, 1969) model to estimate values of primary production.

The Fee (1969) integration of the Vollenweider (1965) primary production model is expressed as

$$\sum_t \sum_Z P = P_{opt}\, \delta \int_{\frac{-\lambda}{2}}^{\frac{\lambda}{2}} \int_{0.01}^{\frac{E(0,t)}{E_k}} \frac{dydt}{\frac{E(0,t)}{E_k}\, k_v(t)\, [(1+y^2)\,(1+(ay)^2)^n]^{0.5}} \qquad (3)$$

where P = rate of photosynthesis per unit area of surface per day

a, n = parameters of the model

P_{opt} = optimum rate of photosynthesis per unit volume of water

$\delta = P_{max}/P_{opt}$ where P_{max} is the maximum rate of photosynthesis per unit volume when a or n = 0

$E(0,t)$ = irradiance just below the surface at time t

$y = E(0,t)/E_k$ where E_k is the light saturation parameter when a or n = 0

λ = day length

$k_v(t)$ = vertical irradiance attenuation coefficient at time t

The limits of integration in equation (3) are, for t, the times of local sunrise and local sunset, and for y, the values corresponding to the surface and the depth of the 1% irradiance level, below which depth no significant contribution to primary production is considered to occur. In Fee's original integration of the Vollenweider model, the vertical irradiance attenuation coefficient $k_v(t)$ was considered to be a constant determined from applying Beer's Law to an irradiance profile. However, as seen from Figure 3 (and discussed in Appendix B), the vertical irradiance attenuation coefficient displays a solar zenith angle dependence, and is therefore a function of time.

Two values of primary production were determined from equation (3), one utilizing the diurnally varying value of $k_v(\theta_r)$ (this integration denoted by $\sum\sum P$) and one utilizing a constant value of k_v (this integration being denoted by $\sum\sum P'$). The difference between these two values of primary production from equation (3) will be referred to herein as the inaccuracy in the determination of primary production by neglecting the solar angle dependence of the vertical irradiance attenuation coefficient. This inaccuracy, expressed as a percentage, is readily given by

$$\% \text{ Inaccuracy} = \left[\frac{\sum\sum P' - \sum\sum P}{\sum\sum P}\right] \cdot 100 \qquad (4)$$

To obtain the constant value of k_v used in these analyses, a value of $k_v(\theta_r)$ was determined for each 10° of solar zenith

angle. Each of these values was considered to represent the constant k_v that would be determined from an irradiance profile taken at that solar zenith angle. These k_v values were then used in equation (3) to yield corresponding $\sum\sum P'$ values. Combining these values of $\sum\sum P'$ with the $\sum\sum P$ values determined using the realistic $k_v(\theta_r)$ dependence of Figure 3 enabled the use of equation (4) to readily determine the inaccuracy as a function of the solar zenith angle existing when an irradiance profile is taken to determine the constant k_v.

Equations (3) and (4) were solved using the half-hour averages obtained in Appendices A and B. The analyses were repeated for three water types (ω = 0.60, ω = 0.75, and ω = 0.90), four times of year [vernal and autumnal equinoxes (March and September) and summer and winter solstices (June and December)] and nine latitudes (10° intervals from 0° to 80°N). Various values of the Vollenweider model parameters a, n, P_{opt}, and E_k and the absorption coefficient were also considered.

b) <u>Determination of Subsurface Irradiation</u>

The irradiance at a depth Z for a subsurface refracted angle θ_r and an incident radiation comprised of both a direct and a diffuse component may be written

$$E(Z,\theta_r) = E(0,\theta_r)\, e^{-k_v(\theta_r)Z} \tag{5}$$

where $k_v(\theta_r)$ = vertical irradiance attenuation coefficient determined in Appendix B

The subsurface irradiation $\Gamma(Z)$ at depth Z for the entire day is obtained by integrating equation (5) over the daylight period.

$$\Gamma(Z) = 2 \int_{\theta_1}^{\theta_2} E(Z,\theta_r)\, d\theta_r$$

$$= 2 \int_{\theta_1}^{\theta_2} E(0,\theta_r)\, e^{-k_v(\theta_r)Z}\, d\theta_r \tag{6}$$

where θ_1 = the subsurface refracted angle for the solar zenith angle at local noon, and

θ_2 = the subsurface refracted angle at sunrise or sunset (48.6° for relative index of refraction of 4/3).

It was assumed that an irradiance profile was taken at a given solar zenith angle and the depths of the 30%, 10%, 3%, and 1% irradiance levels were determined. Irradiation calculations performed for these depths, using the constant k_v obtained from this profile, would give values of 30%, 10%, 3%, and 1%, respectively, of the total daily irradiation just below the surface of the water. It is these values of irradiation that would formerly have been used for a sample incubated at these depths. These values are labelled $\Gamma'(Z)$.

However, in situ incubations performed at these fixed depths throughout the day are not at a fixed subsurface irradiance level. A diurnal variation of the irradiance levels at these depths (Figure 4) due to the solar zenith angle dependence of $k_v(\theta_r)$ would be observed as the levels migrate through these fixed depths. The daily integrated values of these varying irradiances obtained from equation (5) would yield the actual irradiation $\Gamma(Z)$ at depth Z.

In a manner similar to that used for the primary production analysis, the inaccuracy in the determination of irradiation by neglecting the effects of the solar zenith angle dependence of the vertical irradiance attenuation coefficient may be readily defined by:

$$\% \text{ Inaccuracy} = \frac{\Gamma'(Z) - \Gamma(Z)}{\Gamma(Z)} \cdot 100 \qquad (7)$$

Equations (6) and (7) were solved, using half-hour averages, in a manner similar to the solving of equations (3) and (4) for various values of the absorption coefficient, geographic latitude, Julian day, and water type.

DISCUSSION OF INACCURACIES IN ESTIMATION OF PRIMARY PRODUCTION

The percent inaccuracy in the determination of primary production was completely independent of the selection of the Vollenweider parameters a, n, P_{opt}, and E_k as well as the absorption coefficient. It was, however, very dependent upon the selection of ω,

time of year, latitude and the solar zenith angle θ_i when an irradiance profile was taken to determine the constant k_v.

Table 1 lists the inaccuracies determined from equation (4) for latitudes of 0°, 30°N, and 60°N for each of the three water types (ω = 0.60, 0.75, and 0.90) and for the four times of year (March, September, June and December) as a function of solar zenith angle at the time of the constant k_v determination. The inaccuracies observed at the equinoxes (March and September) were invariably identical. Table 1 illustrates that both overestimates (indicated by positive entries) and underestimates (indicated by negative entries) of the primary production may occur. Constant k_v values determined from irradiance profiles performed with the sun nearly vertically overhead (i.e., small values of θ_i) will be characterized by the largest overestimates of primary production while constant k_v values determined from irradiance profiles performed with a rising or setting sun (i.e., large values of θ_i) will be characterized by the largest underestimates of primary production. This is a consequence (see Figure 3) of the determined constant k_v being respectively an underestimate and an overestimate of the average of $k_v(\theta_r)$ for the entire day. Clearly, therefore, there exists some intermediate value of solar zenith angle θ_i at which the determined constant k_v is an appropriate estimate of the average value of $k_v(\theta_r)$ for the entire day. This value of θ_i would be the obvious solar zenith angle at which to perform the irradiance profile. It can be seen from Table 1 that for a fixed latitude and date, such a θ_i value appears

to be independent of water type (i.e., independent of ω). This solar zenith angle for zero inaccuracy, does, however, exhibit a strong dependence on both geographic latitude and Julian day. These dependencies are illustrated in Figure 5 wherein the values of θ_i for zero inaccuracy have been plotted against latitude of observation (degrees North) for the two equinoxes and two solstices. Obvious similarities exist between the equinoxial and winter curves. A distinct difference, however, is noted for the summer curve. This is a direct consequence of the 23.5° tilt of the earth's axis to the plane of the ecliptic.

The last column in Table 1 lists the inaccuracy in the determination of primary production when a constant k_v determined from an irradiance profile taken under totally overcast skies (at any θ_i) is applied to the primary production determinations for clear days. It has been shown (Kirk, 1984) that determining k_v under such overcast conditions is equivalent to determining k_v under clear sky conditions for a solar zenith angle of about 43.5°, and consequently the inaccuracies listed in the last column of Table 1 are comparable with the inaccuracies listed in the 40° and 50° solar zenith angle columns.

The inaccuracies listed in Table 1 are, in general, not large ($<\pm 15\%$), and in most instances quite small ($<\pm 10\%$). Consequently, it is evident that a failure to consider the solar zenith angle dependence of the vertical irradiance attenuation coefficient does not dramatically alter the total daily integrated value of primary

production. However, if the irradiation (irradiance multiplied by incubation time) at a given depth in the water column is required for in situ incubation analysis, then a failure to consider the solar zenith angle dependence of the vertical irradiance attenuation coefficient can produce significant inaccuracies in the estimate of irradiation.

DISCUSSION OF INACCURACIES IN ESTIMATION OF IRRADIATION

Figure 6 displays the inaccuracies in the estimation of irradiation resulting from the assumption of a fixed depth for each of the 30%, 10%, 3%, and 1% irradiance levels for 0° latitude and the March/September equinoxes. These inaccuracies are plotted as a function of the solar zenith angle when the irradiance profile was taken to determine the depths of these irradiance levels. Figure 7 displays these inaccuracies for 0° latitude and the June/December solstices. Both Figures 6 and 7 consider water types defined by ω = 0.60, 0.75, and 0.90. Figure 8 considers the inaccuracy in the estimation of irradiation at a fixed latitude of 30°N for March and June for the 30% and 1% irradiance levels. Again, all 3 water types are shown. Figure 9 considers the inaccuracies associated with the 1% irradiance level at 30°N latitude for all 3 water types throughout the year.

A consideration of Figures 6 to 9 reveals that:

a) The inaccuracies in irradiation determination increase with decreasing values of subsurface irradiance levels (Figures 6 and 7).

b) The inaccuracies vary from a large overestimation of irradiation if the depths of the irradiance levels are determined at small zenith angles to a large underestimation if the depths of the irradiance levels are determined at large zenith angles, passing through a point of zero inaccuracy at some intermediate value of solar zenith angle θ_i (Figures 6, 7, 8 and 9).

c) Each irradiance level has a particular θ_i at which its depth should be determined to result in zero inaccuracy in its irradiation estimate (Figures 6, 7 and 8).

d) The magnitudes of the inaccuracies decrease with increasing ω (Figure 8).

e) The θ_i associated with zero inaccuracy in the determination of irradiation is independent of ω (Figure 9).

f) The relative overestimation or underestimation of irradiation is a function of time of year and the difference between the solar zenith angle when irradiance levels are determined and the solar zenith angle which results in a zero inaccuracy for a given irradiance level (Figure 9).

The relative overestimation or underestimation of irradiation is also a function of geographic latitude. This is illustrated in Figures 10(a) and 10(b) which show the inaccuracy in irradiation determination (for a water mass of $\omega = 0.60$) plotted as a function of the solar zenith angle when the depths of the 30% irradiance level and the 1% irradiance level were determined. Such inaccuracies are shown for latitudes of 0°, 30°N, and 60°N during the equinox and solstice periods. The relative magnitudes of the inaccuracies are clearly seen to be dependent upon the difference between the solar zenith angle at which the depths of the irradiance levels were determined and the solar zenith angle which results in a zero inaccuracy for a given irradiance level. Therefore, to minimize inaccuracies in irradiation determinations, irradiance profiles should be taken at specific solar zenith angles which are dependent upon both latitude and date. This dependence of solar zenith angle for zero inaccuracy upon latitude and date is illustrated in Figure 11 for the 30% and 1% irradiance levels. The values for the 30% irradiance level are identical to the values in Figure 5.

CONCLUSION

The effect of the solar zenith angle dependence of the vertical irradiance attenuation coefficient on the determination of daily primary production is small (<15%) for any latitude and date.

However, this solar zenith angle dependence becomes significant when determining irradiation values for in situ incubations. If daily incubations are considered, then irradiance profiles taken at the solar zenith angles given in Figure 11 provide the best measurements for calculating irradiation. For in situ incubations of shorter time periods, the time dependence of the vertical irradiance attenuation coefficient illustrated in Figure 3 can be effectively utilized to determine a solar zenith angle at which to perform an irradiance profile to estimate a suitable value for the average of $k_v(\theta_r)$.

REFERENCES

Davies, J.A., Schertzer, W. and Nunez, M. 1975. Estimating global radiation. Boundary-Layer Meteorol. 9:33-52.

Fee, E.J. 1969. A numerical model for the estimation of photosynthetic production, integrated over time and depth, in natural waters. Limnol. Oceanogr. 14:906-911.

Jerlov, N.G. 1976. Marine Optics. Elsevier, Amsterdam.

Jerome, J.H., Bruton, J.E. and Bukata, R.P. 1982. Influence of scattering phenomena on the solar zenith angle dependence of in-water irradiance levels. Appl. Opt. 21:642-647.

Kirk, J.T.O. 1984. Dependence of relationship between inherent and apparent optical properties of water on solar altitude. Limnol. Oceanogr. 29(2):350-356.

Patten, B.C. 1968. Mathematical models of plankton production. Int. Rev. Gesamten Hydrobiol. 53:357-408.

Smith, E.L. 1936. Photosynthesis in relation to light and carbon dioxide. Proc. Natl. Acad. Sci. U.S. 22:504.

Talling, J.F. 1957. The phytoplankton population as a compound photosynthetic system. New Phytologist 56:133-149.

Vollenweider, R.A. 1965. Calculation models of photosynthesis-depth curves and some implications regarding day rate estimates in primary production measurements. Mem. Ist. Ital. Idrobiol. 18 (Suppl):425-457.

APPENDIX A: THE INCIDENT RADIATION FIELD

The incident radiation field considered in this analysis was taken to be comprised of a direct solar beam superimposed upon a diffuse radiation distribution emanating from the sky. Obviously, on any given day, such an incident radiation distribution can display large variations, ranging from nearly totally direct to totally diffuse. The effects of such variations in incident radiation distributions on the depths of subsurface irradiance levels have been discussed elsewhere (Jerome et al., 1982). For the purpose of this work, we have considered an incident radiation field determined from the clear-day global radiation model of Davies et al., (1975). On the basis of this model, a direct solar irradiance E_{sun} and a diffuse sky irradiance E_{sky} were obtained from

$$E_{sun} = (E_{sol} \cos \theta_i) \psi_{WA} \psi_{DA} \psi_{WS} \psi_{RS} \psi_{DS}/R^2 \qquad (A1)$$

$$E_{sky} = (E_{sol} \cos \theta_i) \psi_{WA} \psi_{DA} (1-\psi_{WS} \psi_{RS} \psi_{DS})/2R^2 \qquad (A2)$$

where E_{sol} = solar irradiance at the mean annual earth-sun distance (i.e., at 1 Astronomical Unit)

θ_i = solar zenith angle

R = radius vector (expressed in Astronomical Units)

and ψ_{WA}, ψ_{DA}, ψ_{WS}, ψ_{DS} and ψ_{RS} are atmospheric parameters which account for absorption and scattering effects of atmospheric water and dust, and Rayleigh scattering. These parameters are obtained from air mass and precipitable water content of the atmosphere in the manner described by Davies et al., (1975). Table 2 lists the diffuse fraction F of the total incident irradiance as a function of solar zenith angle used in this analysis. Table 2 was constructed assuming a precipitable water content of 1.5 cm, a value which reasonably approximates the range of atmospheric conditions normally encountered. It should be emphasized that Table 2 represents a clear-day atmosphere.

The direct and diffuse incident irradiances E_{sun} and E_{sky} were determined as a function of time from sunrise to sunset. These incident irradiance values were taken through the air/water interface to obtain values of the irradiance $E(0,\theta_r)$ just below the water surface. Surface reflection of the direct component E_{sun} was obtained from the angular dependency of the Fresnel reflectivity. Surface reflection of the diffuse component E_{sky} was taken to be 0.066 (Jerlov, 1976). Such surface reflection results in the diffuse fraction of the subsurface irradiance $E(0,\theta_r)$ being slightly different from the diffuse fraction F of the above-water incident irradiance. This slightly different subsurface diffuse fraction will

be denoted as F_w and the F_w values are also listed in Table 2. Half-hour averages of the subsurface irradiance $E(0,\theta_r)$ were determined from sunrise to sunset and these half-hour averages were used in the integrations of equations (3) and (6).

APPENDIX B: DETERMINATION OF DIURNAL VARIATION OF THE VERTICAL IRRADIANCE ATTENUATION COEFFICIENT, $k_v(\theta_r)$

Using a Monte Carlo simulation of photon propagation through natural waters, Kirk (1984) has presented empirical relationships relating the vertical irradiance attenuation coefficient to time of day and water type. These empirical relationships may be expressed as

$$k_{vsun}(\theta_r) = \frac{1}{\cos\theta_r}\left[a^2 + (0.425\cos\theta_r - 0.190)ab\right]^{\frac{1}{2}} \qquad \text{(B1)}$$

$$k_{vsky} = 1.168\left[a^2 + 0.162ab\right]^{\frac{1}{2}} \qquad \text{(B2)}$$

where

$k_{vsun}(\theta_r)$ = vertical irradiance attenuation coefficient for the direct component of $E(0,\theta_r)$

k_{vsky} = vertical irradiance attenuation coefficient for the diffuse component of $E(0,\theta_r)$

θ_r = in-water refracted angle

a = absorption coefficient of the water

b = scattering coefficient of the water

In this work we have combined Kirk's equations into a single relationship which can be used to obtain the solar zenith angle dependence of $k_v(\theta_r)$ for the subsurface radiation distribution of Table 2 and a variety of natural waters. This single combined relationship may be written as

$$k_v(\theta_r) = F_w k_{vsky} + (1-F_w)k_{vsun}(\theta_r) \qquad \text{(B3)}$$

where F_w = fraction of the subsurface irradiance that is diffuse

Kirk (1984) optically distinguishes natural waters by means of the absorption and scattering coefficients a and b. In this work, however, we have distinguished natural waters in terms of the absorption coefficient and the scattering albedo ω [defined as the ratio b/(a+b) and representing that proportion of photon interactions in the water that are scattering events]. Three different water types were considered, characterized by $\omega = 0.60$, $\omega = 0.75$ and $\omega = 0.90$, each of the three water types displaying a progressively higher percentage of scattering interactions.

The solar zenith angle dependence of the vertical irradiance attenuation coefficient is illustrated in Figure 3 for the three ω values and the incident radiation distribution given by Table 2. Two

features are evident from Figure 3: (i) as ω increases, the solar zenith angle dependence of $k_v(\theta_r)$ decreases; and (ii) the relative value of $k_v(\theta_r)$ (for all values of ω) increases with increasing solar zenith angles up to ~70° at which point the relative value of $k_v(\theta_r)$ decreases. This decrease in the relative value of $k_v(\theta_r)$ at large solar zenith angles is due to the rapidly increasing percentage of diffuse radiation in the total incident radiation observed for large solar zenith angles.

The time dependence of $k_{vsun}(\theta_r)$ and $kv(\theta_r)$ were obtained throughout the entire day. From this time dependence, half-hour averages of $k_v(\theta_r)$ between sunrise and sunset were readily obtained. These half-hour averages were used in the integrations of equations (3) and (6).

TABLE CAPTIONS

Table 1. Percent inaccuracies, from using a constant k_v, in the estimation of daily primary production.

Table 2. Incident radiation distribution as a function of solar zenith angle.

Table 1.

Latitude and Date	Solar Zenith Angle at Time of k_v Determination									Totally Diffuse
	0°	10°	20°	30°	40°	50°	60°	70°	80°	
0°										
March/September										
ω = 0.60	8	7	5	1	-3	-8	-12	-14	-13	-4
ω = 0.75	6	6	4	1	-2	-6	-9	-12	-11	-3
ω = 0.90	4	4	3	1	-2	-4	-6	-8	-7	-4
June/December										
ω = 0.60			8	4	0	-5	-9	-12	-10	-1
ω = 0.75			6	3	0	-4	-7	-10	-9	-1
ω = 0.90			4	2	0	-3	-5	-6	-6	-2
30°N										
March/September										
ω = 0.60			10	6	2	-3	-8	-10	-9	1
ω = 0.75			8	5	1	-3	-6	-9	-8	0
ω = 0.90			5	3	1	-2	-4	-5	-5	-1
June										
ω = 0.60	9	8	5	2	-3	-7	-11	-14	-13	-3
ω = 0.75	7	6	4	1	-2	-6	-9	-11	-10	-3
ω = 0.90	5	4	3	1	-1	-4	-6	-7	-7	-3
December										
ω = 0.60						4	0	-4	-2	9
ω = 0.75						4	0	-3	-2	7
ω = 0.90						2	0	-2	-2	3
60°N										
March/September										
ω = 0.60						6	1	-2	0	11
ω = 0.75						5	1	-1	1	8
ω = 0.90						3	1	-1	-1	4
June										
ω = 0.60				9	4	-1	-6	-8	-7	3
ω = 0.75				7	3	-1	-4	-7	-6	2
ω = 0.90				4	2	0	-3	-4	-4	0
December										
ω = 0.60									-5	6
ω = 0.75									-4	5
ω = 0.90									-2	2

Table 2.

Solar Zenith Angle (degrees)	Diffuse Fraction of Above Surface Irradiance F	Diffuse Fraction of Subsurface Irradiance F_w
0	0.080	0.077
10	0.081	0.078
20	0.084	0.080
30	0.090	0.086
40	0.100	0.096
50	0.116	0.113
60	0.147	0.146
70	0.216	0.229
80	0.439	0.529
90	1.000	1.000

FIGURE CAPTIONS

Figure 1. Ray diagram illustrating the passage of incident radiation into the water column.

Figure 2. Flow diagram of the methodology used to determine the inaccuracies in the estimation of irradiation and primary production resulting from ignoring the diurnal variation of the vertical irradiance attenuation coefficient.

Figure 3. Solar zenith angle dependence of k_v for water masses defined by $\omega = 0.60$, $\omega = 0.76$, and ω 0.90

Figure 4. The relative depth of the 30%, 10%, 3%, and 1% subsurface irradiance levels as a function of solar zenith angle
a) for a water mass defined by $\omega = 0.60$ and $k_v(0°) = 1.0\ m^{-1}$
b) for a water mass defined by $\omega = 0.90$ and $k_v(0°) = 1.0\ m^{-1}$

Figure 5. The solar zenith angle at the time of k_v determination for a zero inaccuracy in the determination of daily primary production as a function of latitude of observation for different times of year.

Figure 6. The percent inaccuracies in the estimation of irradiation for each of the 30%, 10%, 3%, and 1% irradiance levels for 0° latitude and the March/September equinoxes.

Figure 7. The percent inaccuracies in the estimation of irradiation for each of the 30%, 10%, 3%, and 1% irradiance levels for 0° latitude and the June/December solstices.

Figure 8. The percent inaccuracies in the estimation of irradiation for the 30% and 1% irradiance levels at 30°N latitude in March and June.

Figure 9. The percent inaccuracies in the estimation of irradiation for the 1% irradiance levels at 30°N latitude for all three considered water types throughout the year.

Figure 10. The percent inaccuracy in the determination of irradiation for three latitudes

a) for the 30% irradiance level and a water mass defined by $\omega = 0.60$

b) for the 1% irradiance level and a water mass defined by $\omega = 0.60$

Figure 11. The solar zenith angle at the time of k_v determination for zero inaccuracy in the determination of irradiation as a function of latitude in June, March/September, and December.

Figure 1

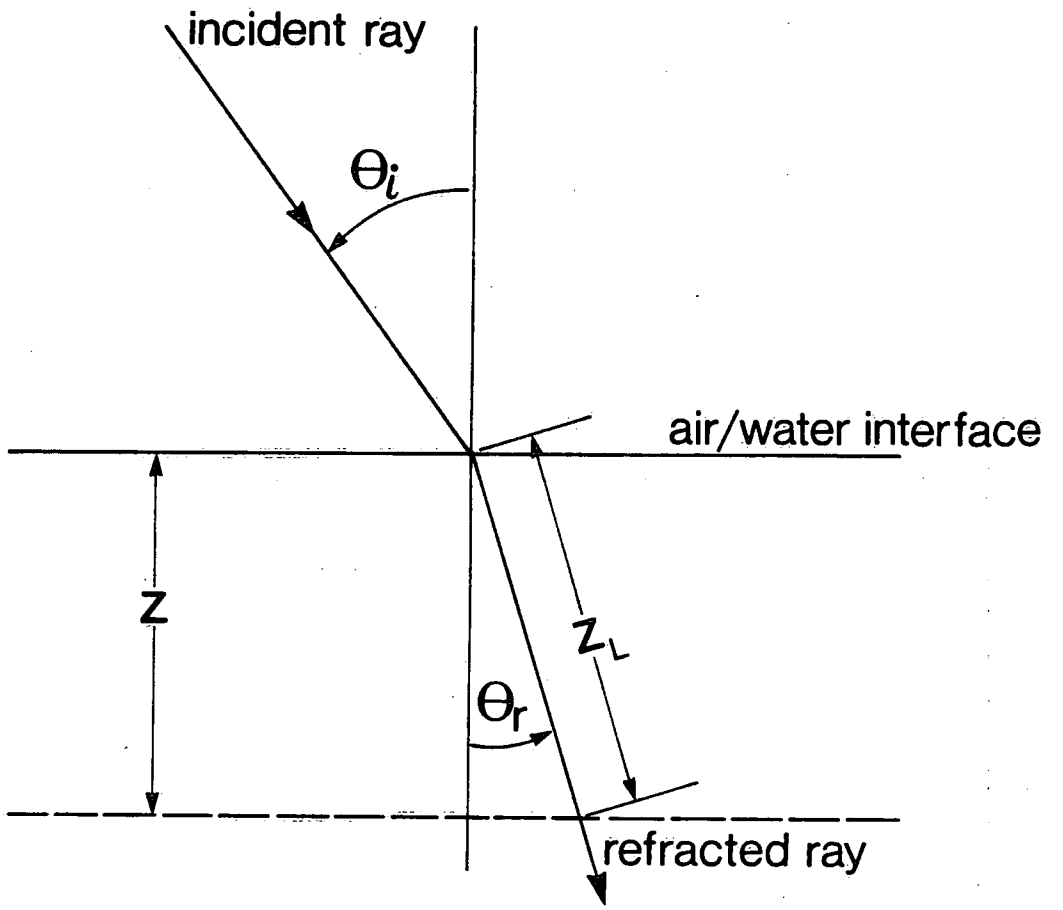
incident ray
θ_i
air/water interface
Z
Z_L
θ_r
refracted ray

Figure 2

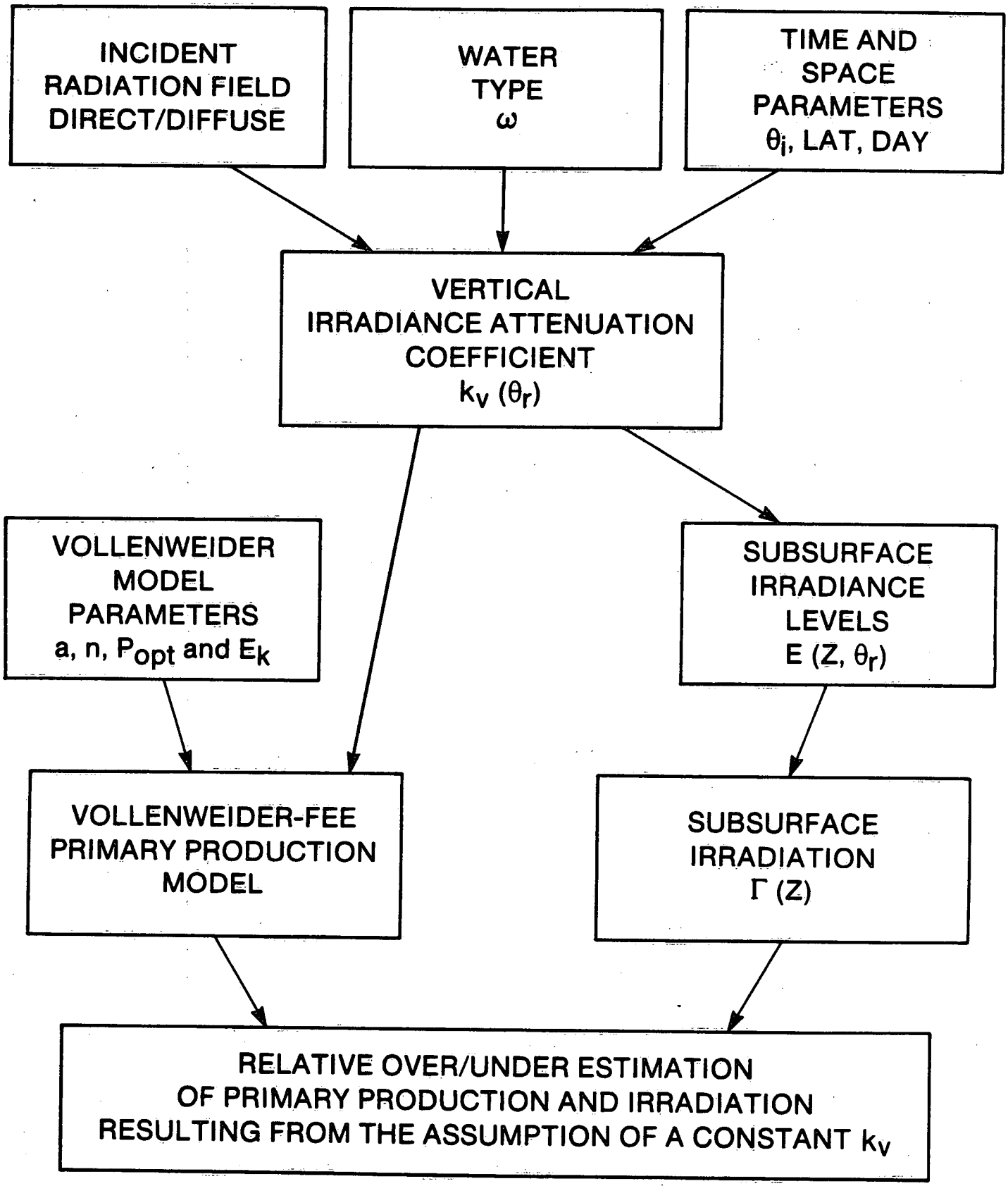
INCIDENT RADIATION FIELD DIRECT/DIFFUSE
WATER TYPE ω
TIME AND SPACE PARAMETERS θi, LAT, DAY
VERTICAL IRRADIANCE ATTENUATION COEFFICIENT kv (θr)
VOLLENWEIDER MODEL PARAMETERS a, n, Popt and Ek
SUBSURFACE IRRADIANCE LEVELS E (Z, θr)
VOLLENWEIDER-FEE PRIMARY PRODUCTION MODEL
SUBSURFACE IRRADIATION Γ (Z)
RELATIVE OVER/UNDER ESTIMATION OF PRIMARY PRODUCTION AND IRRADIATION RESULTING FROM THE ASSUMPTION OF A CONSTANT kv

Figure 3

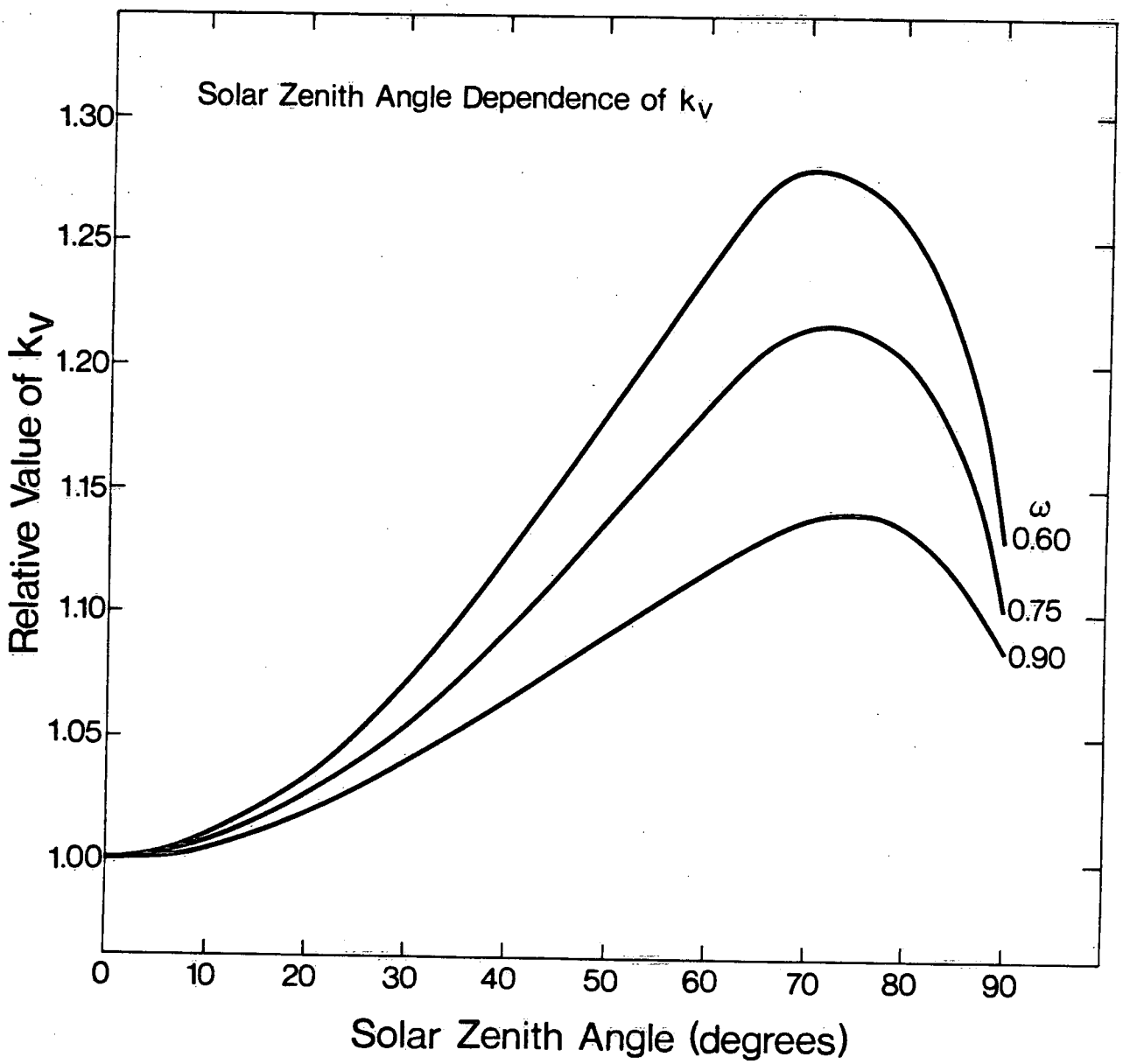
Solar Zenith Angle Dependence of k_V
Relative Value of k_V
1.30
1.25
1.20
1.15
1.10
1.05
1.00
0
10
20
30
40
50
60
70
80
90
Solar Zenith Angle (degrees)
ω
0.60
0.75
0.90

Figure 4

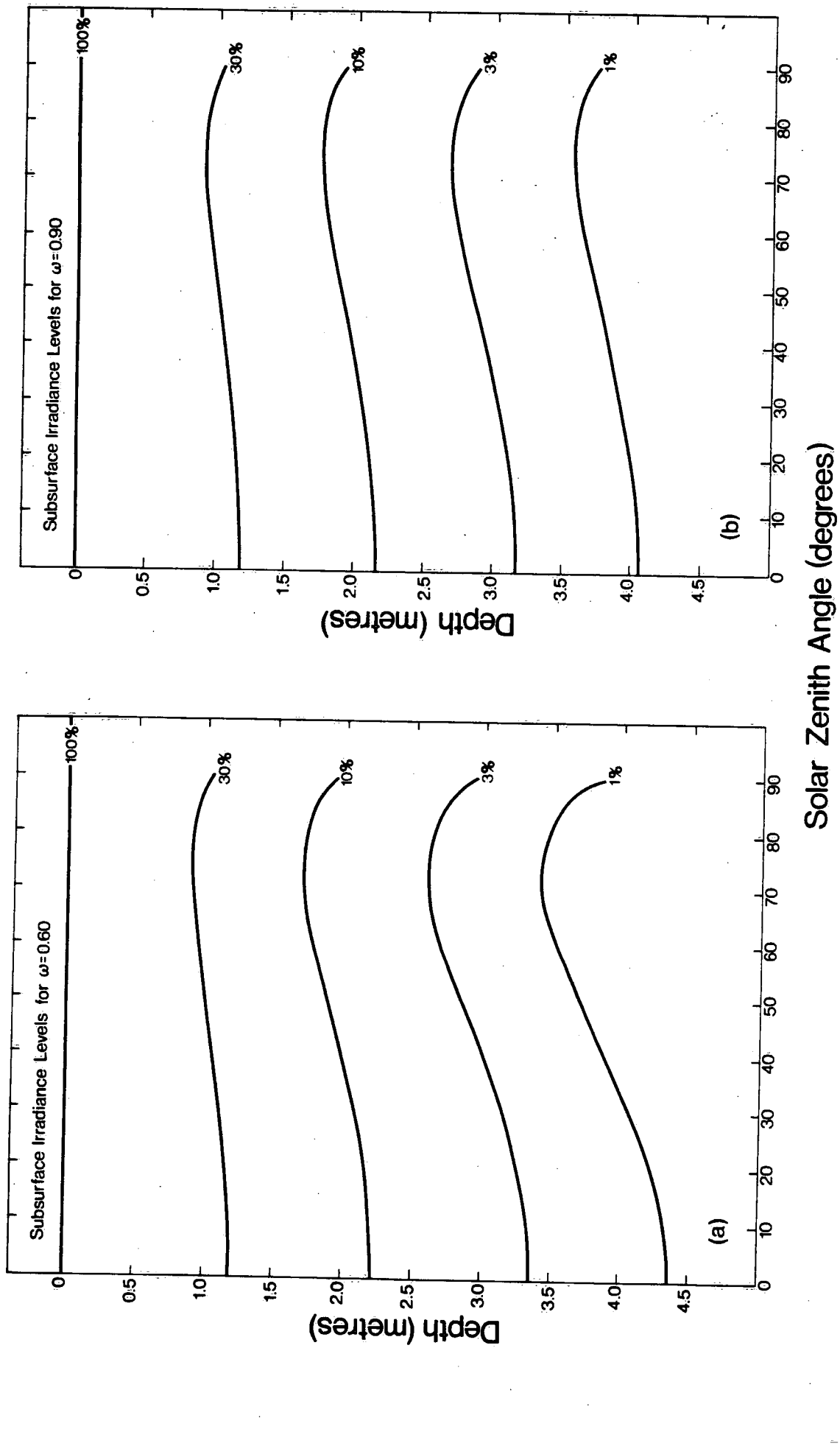
Subsurface Irradiance Levels for ω=0.60
Subsurface Irradiance Levels for ω=0.90
100%
30%
10%
3%
1%
Depth (metres)
Solar Zenith Angle (degrees)
(a)
(b)
0
0.5
1.0
1.5
2.0
2.5
3.0
3.5
4.0
4.5
10
20
30
40
50
60
70
80
90

Figure 5

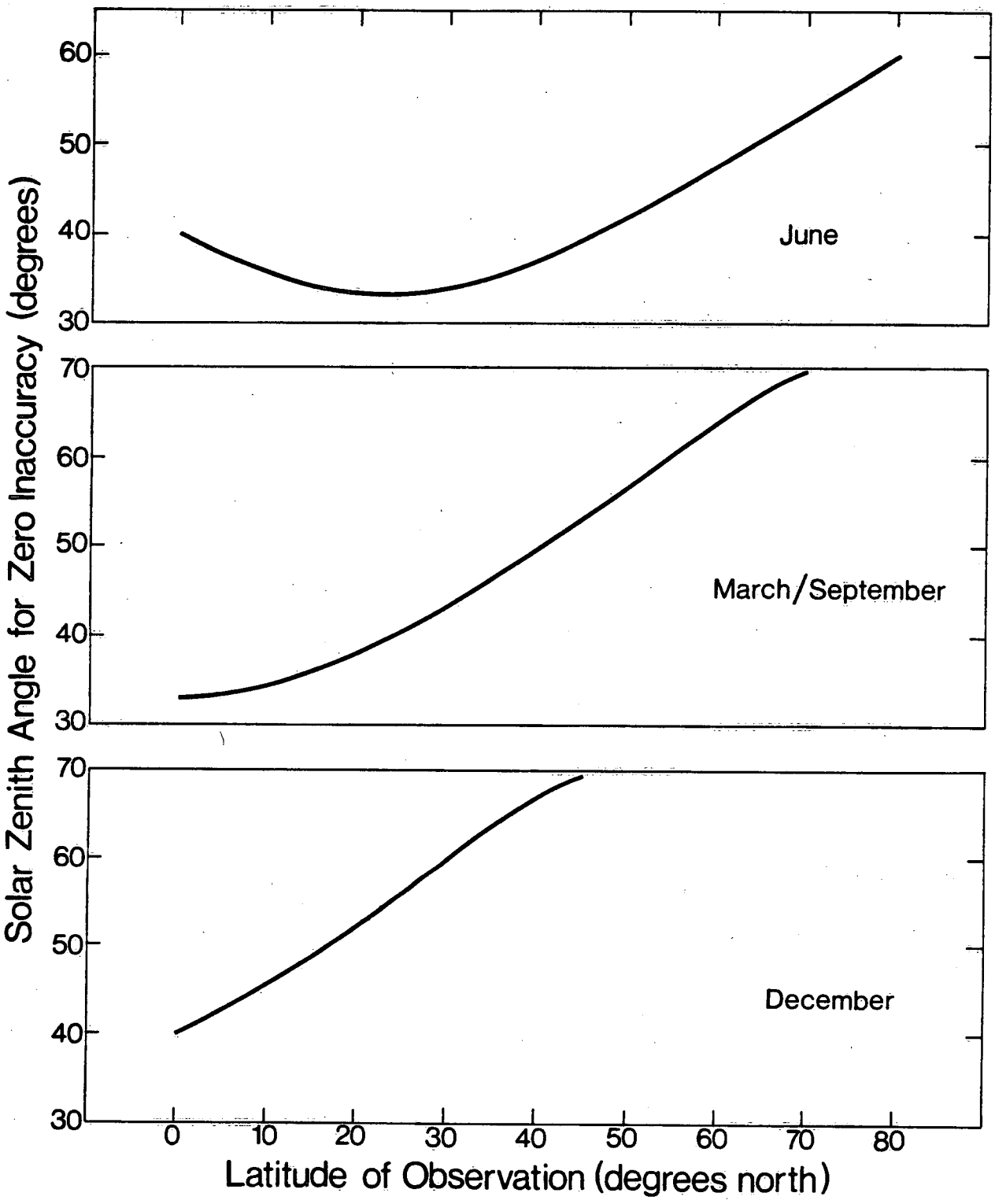
Solar Zenith Angle for Zero Inaccuracy (degrees)
60
50
40
30
June
70
60
50
40
30
March/September
70
60
50
40
30
December
0
10
20
30
40
50
60
70
80
Latitude of Observation (degrees north)

Figure 6

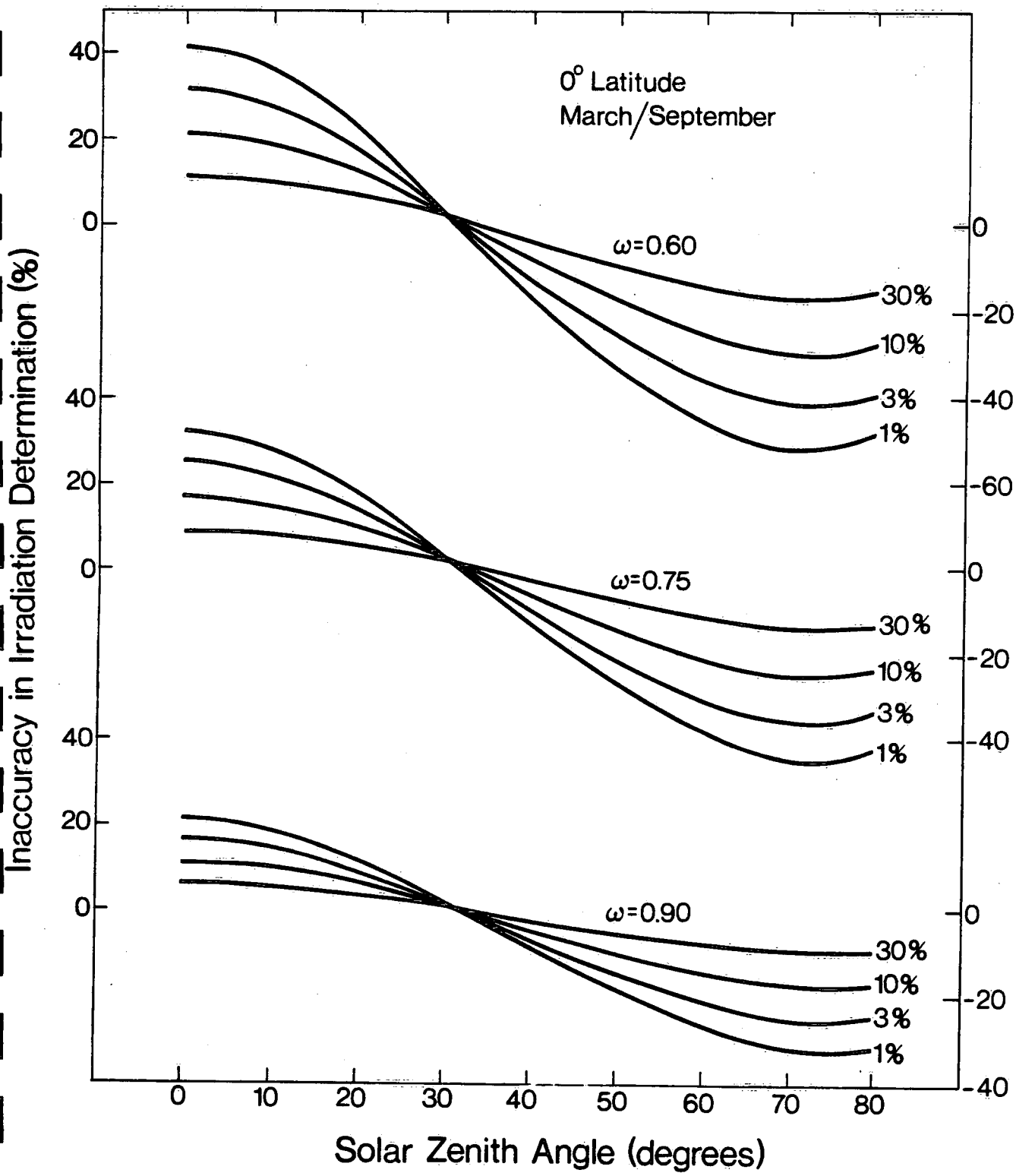
0° Latitude
March/September
ω=0.60
ω=0.75
ω=0.90
30%
10%
3%
1%
Inaccuracy in Irradiation Determination (%)
Solar Zenith Angle (degrees)
0
10
20
30
40
50
60
70
80
-20
-40
-60

Figure 7

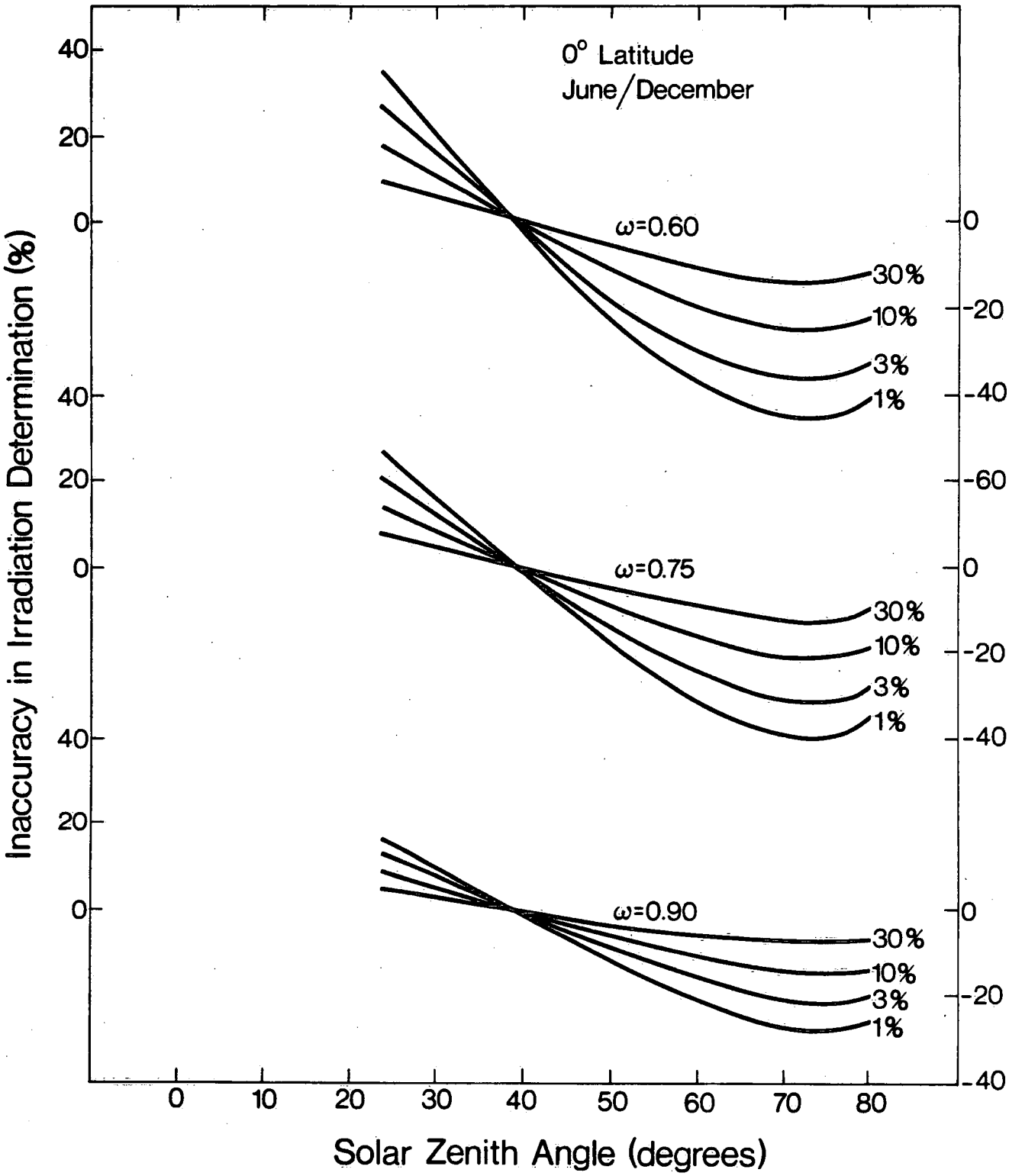
0° Latitude
June/December
ω=0.60
30%
10%
3%
1%
ω=0.75
30%
10%
3%
1%
ω=0.90
30%
10%
3%
1%
Inaccuracy in Irradiation Determination (%)
Solar Zenith Angle (degrees)
40
20
0
40
20
0
40
20
0
0
-20
-40
-60
0
-20
-40
0
-20
-40
0
10
20
30
40
50
60
70
80

Figure 8

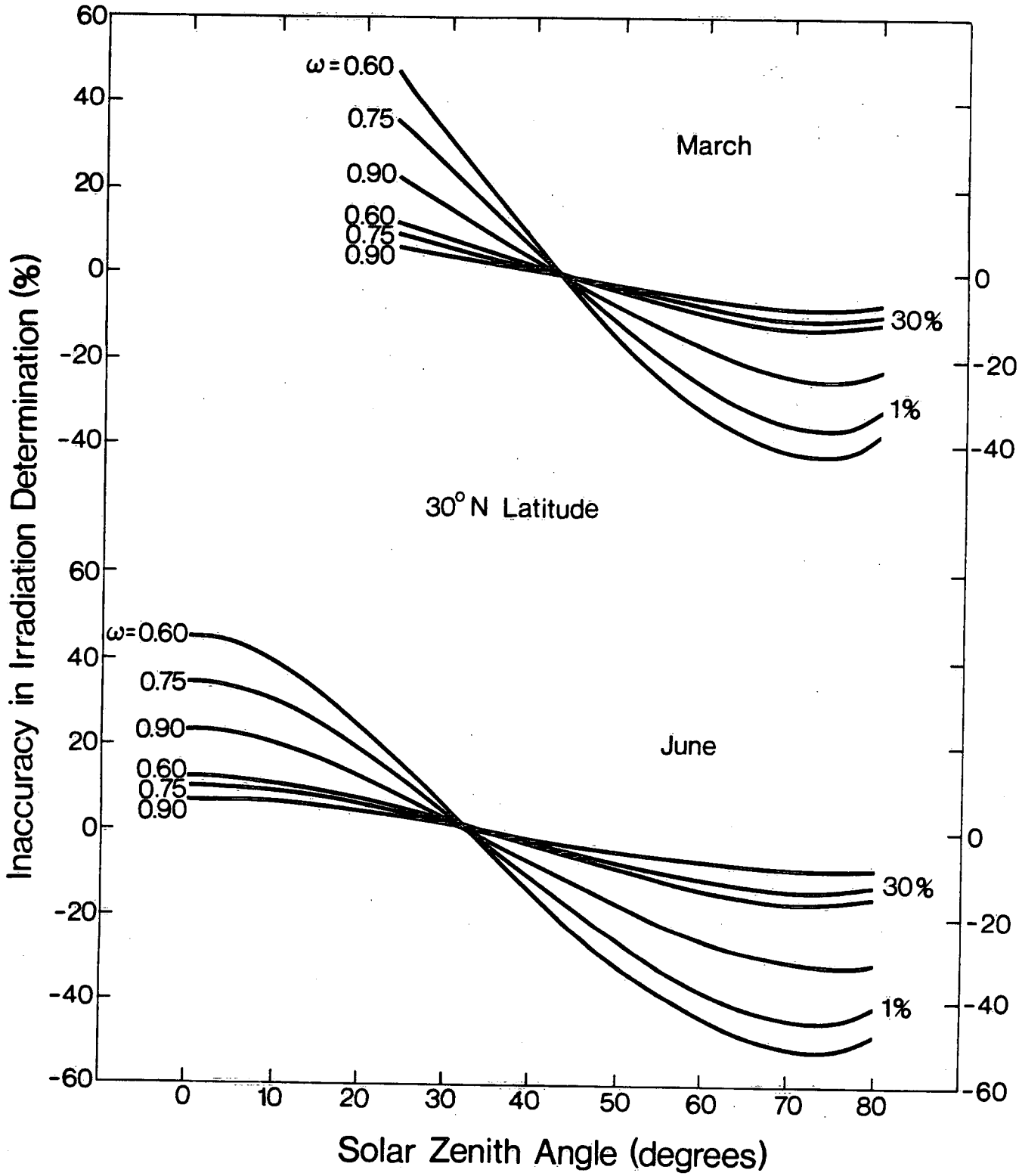
ω=0.60
0.75
0.90
March
0.60
0.75
0.90
30%
1%
30° N Latitude
ω=0.60
0.75
0.90
June
0.60
0.75
0.90
30%
1%
Inaccuracy in Irradiation Determination (%)
Solar Zenith Angle (degrees)
60
40
20
0
-20
-40
-60
0
10
20
30
40
50
60
70
80

Figure 9

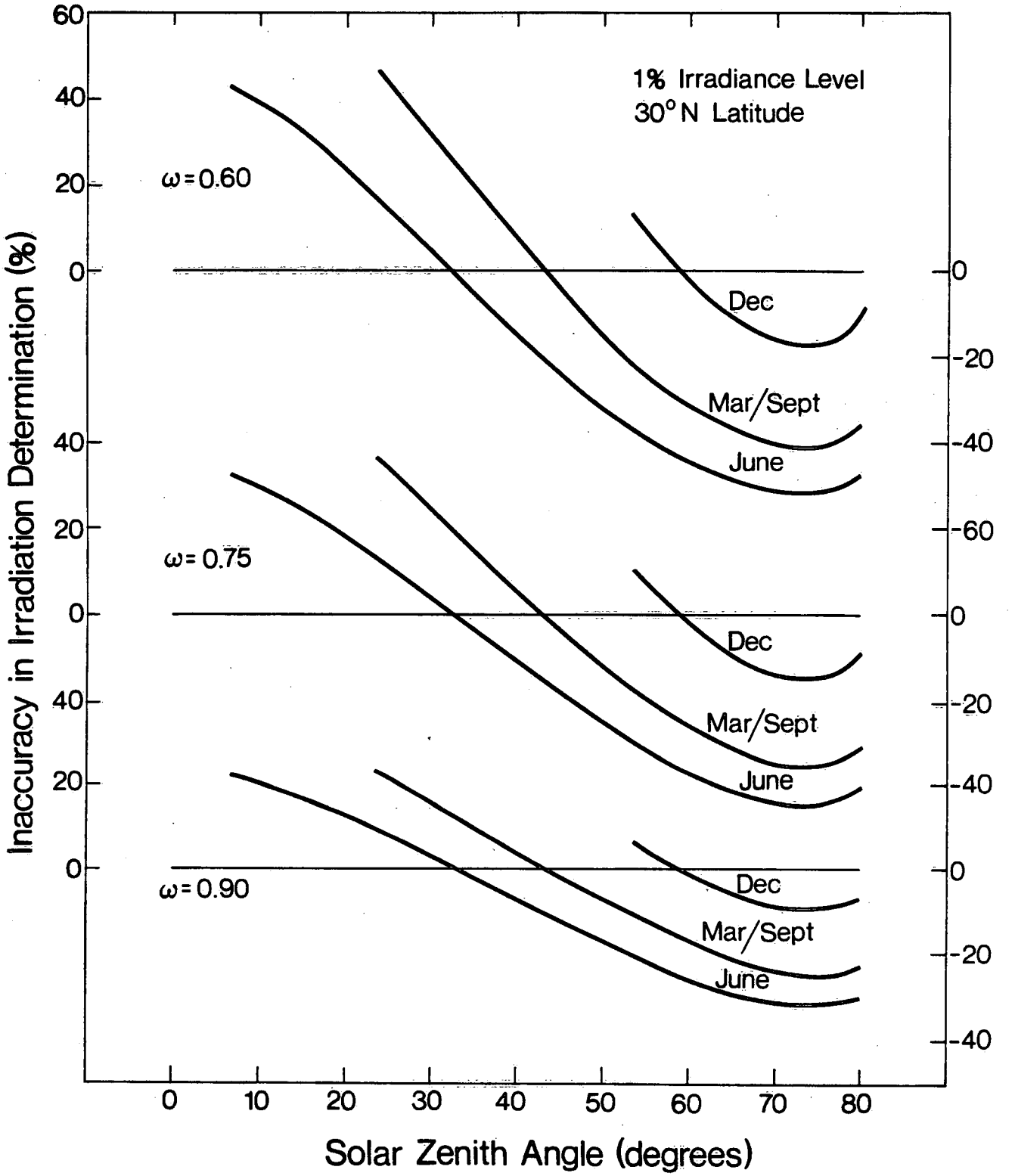
1% Irradiance Level
30° N Latitude
ω = 0.60
ω = 0.75
ω = 0.90
Dec
Mar/Sept
June
Inaccuracy in Irradiation Determination (%)
Solar Zenith Angle (degrees)
60
40
20
0
-20
-40
-60
0
10
20
30
40
50
60
70
80

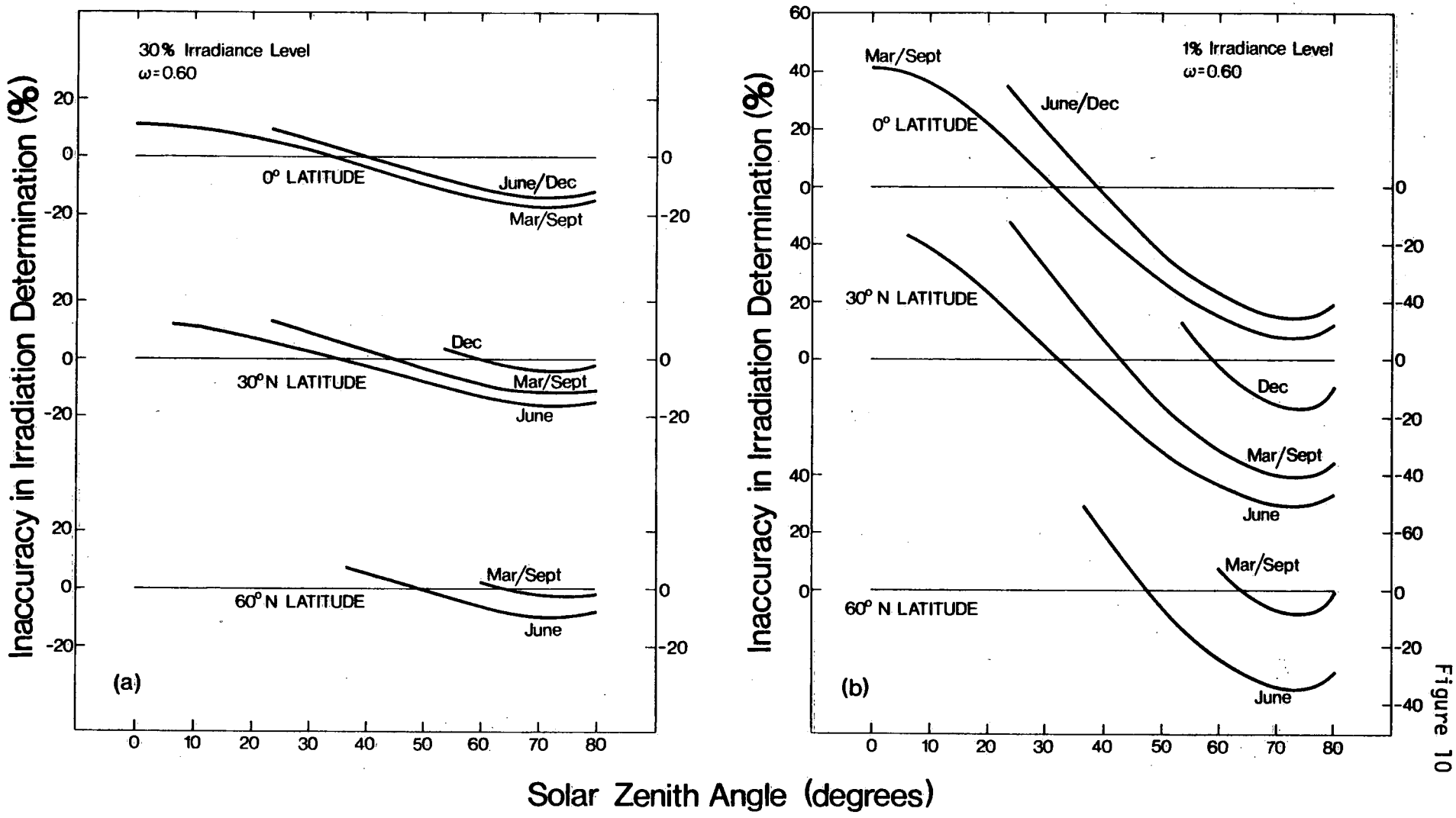
30% Irradiance Level
ω=0.60
0° LATITUDE
June/Dec
Mar/Sept
30°N LATITUDE
Dec
Mar/Sept
June
60° N LATITUDE
Mar/Sept
June
(a)
1% Irradiance Level
ω=0.60
Mar/Sept
0° LATITUDE
June/Dec
30° N LATITUDE
Dec
Mar/Sept
June
60° N LATITUDE
Mar/Sept
June
(b)
Inaccuracy in Irradiation Determination (%)
Solar Zenith Angle (degrees)

Figure 10

Figure 11

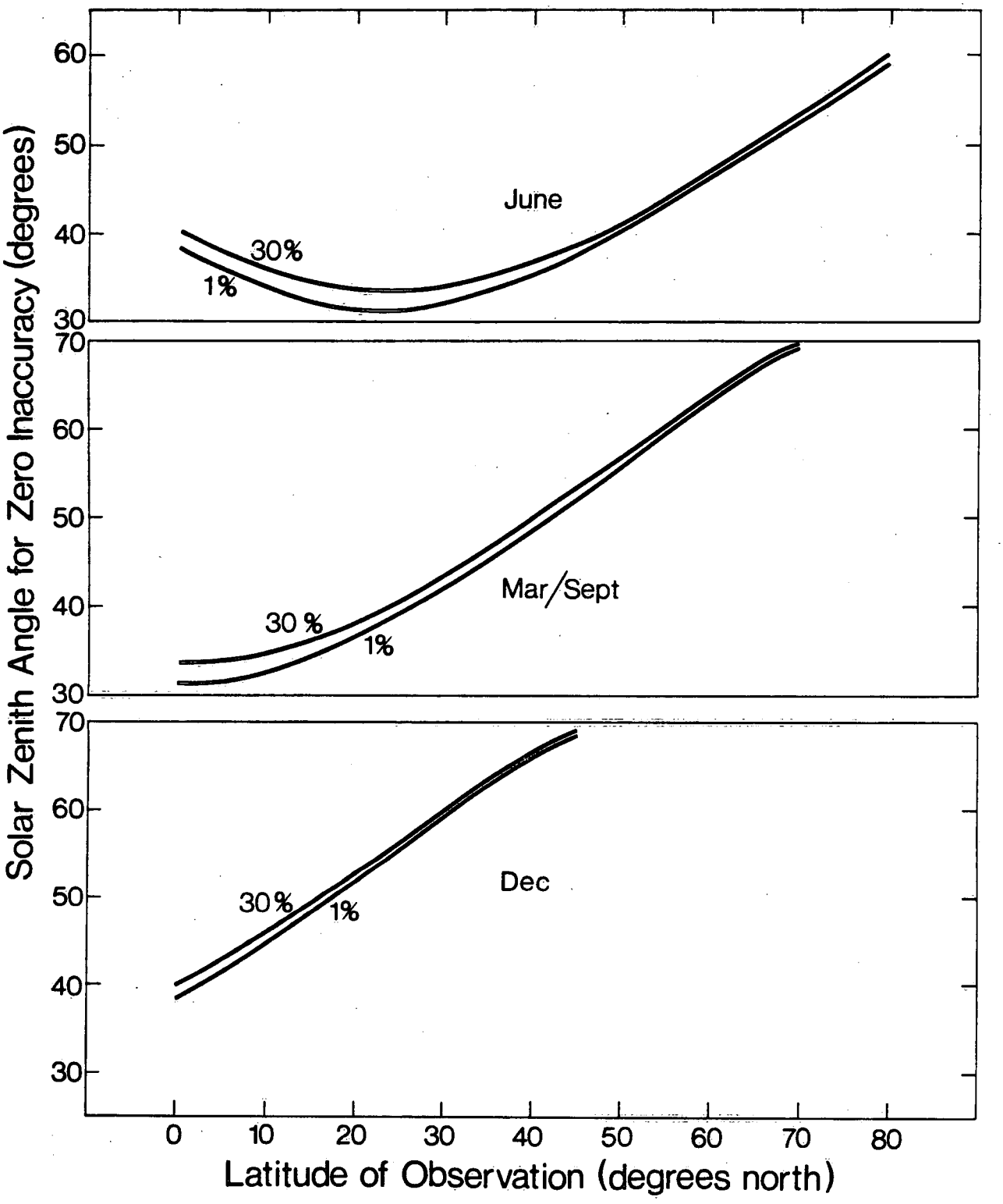
Solar Zenith Angle for Zero Inaccuracy (degrees)
60
50
40
30
June
30%
1%
70
60
50
40
30
Mar/Sept
30 %
1%
70
60
50
40
30
Dec
30%
1%
0
10
20
30
40
50
60
70
80
Latitude of Observation (degrees north)